nature geoscience

SUPPLEMENTARY INFORMATION

DOI: 10.1038/NGEO1744

Increase in the Range between Wet and Dry Season Precipitation

Chia Chou, John C. H. Chiang, Chia-Wei Lan, Chia-Hui Chung, Yi-Chun Liao and Chia-Jung Lee

TABLE S1: A list of the 23 coupled atmosphere-ocean climate models from the CMIP3 archive used in this study.

Model	Description
AUS_CSIRO_MK3	Commonwealth Scientific and Industrial Research Organisation Mark, CSIRO model V3 (Australia)
AUT_CSIRO_MK3.5	Commonwealth Scientific and Industrial Research Organisation Mark, CSIRO model V3.5 (Australia)
CA_CCCMA3.1_T47	Canadian Centre for Climate Modelling and Analysis, CGCM3.1 Model (T47) (Canada)
CA_CCCMA3.1_T63	Canadian Centre for Climate Modelling and Analysis CGCM3.1 Model (T63) (Canada)
CN_IAP	LASG, Institute of Atmospheric Physics, FGOALS1.0_g Model (China)
FR_CNRM_CM3	Centre National de Research Meteorologiques, CM3 Model (France)
FR_IPSL_CM4.1	IPSL/LMD/LSCE, CM4 V1 Model (France)
GFDL_CCM2.0	NOAA Geophysical Fluid Dynamics Laboratory, CM2.0 Model (United States)
GFDL_CCM2.1	NOAA Geophysical Fluid Dynamics Laboratory, CM2.1 Model (United States)
GISS_AOM	NASA Goddard Institute for Space Studies, GISS_AOM model (United States)
GISS_EH	NASA Goddard Institute for Space Studies, GISS_EH model (United States)
INGV_ECHAM4	Instituto Nazionale di Geofisica e Vulcanologia, INGV_SXG (SINTEX-G) model (Italy)
JP_CCSR3.2H	CCSR/NIES/FRCGC, MIROC Model V3.2, high resolution (Japan)
JP_CCSR3.2M	CCSR/NIES/FRCGC, MIROC Model V3.2, medium resolution (Japan)
JP_MRI2.3	Meteorological Research Institute (MRI), CM2.3.2a (Japan)
MPI_ECHAM5	Max Planck Institute for Meteorology, ECHAM5/MPI OM (Germany)
MUB_ECHOG	Meteorological Institute of the University of Bonn, Meteorological Research Institute of KMA, ECHOG model (Germany/Korea)

TABLE S1: Continued.

Model	Description
NCAR_CCSM3	NCAR Community Climate System Model, CCSM3.0 (United States)
NCAR_PCM1	NCAR Parallel Climate Model (Version 1) (United States)
BCCR_BCM2	Bjerknes Centre for Climate Research, Bergen Climate Model (BCM) V2 (Norway)
Russia_INMCM3	Institute for Numerical Mathematics, INMCM3.0 Model (Russia)
UKMO_HadCM3	Hadley Center for Climate Prediction, Met Office, HadCM3 Model (United Kingdom)
UKMO_HadGEM1	Hadley Centre for Climate Prediction, Met Office, HadGEM1 Model (United Kingdom)

TABLE S2: A list of the 18 coupled atmosphere-ocean climate models from the CMIP5 archive used in this study.

Model	Institution
BBC-CSM1.1	Beijing Climate Center, China Meteorological Administration
CanESM2	Canadian Centre for Climate Modelling and Analysis
CCSM4	National Center for Atmospheric Research
FGOALS-g2	LASG, Institute of Atmospheric Physics, Chinese Academy of Sciences; and CESS, Tsinghua University
FGOALS-s2	LASG, Institute of Atmospheric Physics, Chinese Academy of Sciences
GFDL-CM3	Geophysical Fluid Dynamics Laboratory
GFDL-ESM2G	Geophysical Fluid Dynamics Laboratory
GFDL-ESM2M	Geophysical Fluid Dynamics Laboratory
GISS-E2-R	NASA Goddard Institute for Space Studies
HadGEM2-CC	Met Office Hadley Centre
INM-CM4	Institute for Numerical Mathematics
IPSL-CM5A-LR	Institut Pierre-Simon Laplace
MIROC5	Atmosphere and Ocean Research Institute (The University of Tokyo), National Institute for Environmental Studies, and Japan Agency for Marine-Earth Science and Technology
MIROC-ESM	Atmosphere and Ocean Research Institute (The University of Tokyo), National Institute for Environmental Studies, and Japan Agency for Marine-Earth Science and Technology
MIROC-ESM-CHEM	Atmosphere and Ocean Research Institute (The University of Tokyo), National Institute for Environmental Studies, and Japan Agency for Marine-Earth Science and Technology
MPI-ESM-LR	Max Planck Institute for Meteorology (MPI-M)
MRI-CGCM3	Meteorological Research Institute
NorESM1-M	Norwegian Climate Centre

TABLE S3: Pattern correlations of precipitation changes between the evaluation periods of 1979-2010 and 1988-2010 and between the original data and the corresponding first EOF for wet seasons, dry seasons and the annual range in GPCP and SSM/I.

Data	**wet**	**Dry**	**annual range**
1979-2010 original (GPCP) vs. 1988-2010 original (GPCP)	0.70	0.66	0.63
1979-2010 original (GPCP) vs. 1979-2010 1st EOF (GPCP)	0.87	0.86	0.91
1988-2010 original (GPCP) vs. 1988-2010 1st EOF (GPCP)	0.65	0.78	0.65
1988-2010 original (GPCP) vs. 1988-2010 original (SSM/I)	0.54	0.65	0.52
1988-2010 1st EOF (GPCP) vs. 1988-2010 1st EOF (SSM/I)	0.82	0.81	0.77

TABLE S4: Trends of globally averaged precipitation in wet and dry seasons, and the annual precipitation range in the period of 1979-2010 for the 23 CMIP3 climate model (Table S1) simulations in the A1B scenario, combined with the 20C3M runs. One realization from each model is chosen. The spatial coverage includes global and land-only. The unit is % per 1˚C. The trends that passed the 95% statistical confidence level of a two-tailed t test are marked in bold font.

Model	**wet**		**dry**		**annual range**	
coverage	global	land	global	land	global	land
ensemble	**2.91**	**3.21**	-0.28	1.34	**3.35**	**2.85**
AUS_CSIRO_MK3	4.75	12.97	4.84	9.51	3.64	**10.61**
AUS_CSIRO_MK3.5	**3.96**	1.35	-1.04	15.93	4.45	0.37
CA_CCCMA3.1_T47	**4.36**	**4.03**	1.78	2.66	**2.86**	2.31
CA_CCCMA3.1_T63	**1.84**	**2.86**	**2.80**	**4.49**	0.90	1.76
CN_IAP	-0.29	-5.12	1.62	6.57	-1.45	**-8.40**
FR_CNRM_CM3	1.86	1.93	-1.45	-0.33	3.36	2.40
FR_IPSL_CM4.1	**3.59**	2.06	-1.27	-0.66	**5.29**	2.53
GFDL_CCM2.0	2.54	2.70	-0.67	2.84	3.04	2.31
GFDL_CCM2.1	2.42	2.02	-0.08	4.98	2.72	1.13
GISS_AOM	1.22	3.84	1.21	-3.76	0.86	**6.99**
GISS_EH	**15.01**	**15.07**	**-9.32**	**-9.39**	**23.11**	**17.55**
INGV_ECHAM4	**3.14**	-0.15	-1.04	-2.60	**4.62**	0.32
JP_CCSR3.2M	1.89	3.60	1.49	3.85	1.54	2.74
JP_CCSR3.2H	**2.13**	**2.14**	0.45	-0.21	**2.53**	2.41
JP_MRI2.3	7.32	**13.51**	**-9.72**	-3.78	**13.58**	**15.14**
MPI_ECHAM5	6.11	2.39	-6.48	6.31	8.18	0.74
MIUB_ECHOG	1.92	**3.38**	0.66	2.40	2.04	3.13
NCAR_CCSM3	**1.78**	**4.57**	2.00	3.05	1.77	**5.04**
NCAR_PCM1	**4.78**	**6.72**	-0.25	-0.21	**4.45**	**5.69**
NW_BCCR_CM2	**4.99**	5.15	-0.69	1.57	5.45	3.90
Russia_INMCM3	2.41	2.96	0.57	1.34	2.29	2.36
UKMO_HadCM3	-0.89	0.25	2.91	1.24	-2.30	-0.08
UKMO_HadGEM1	1.60	3.08	2.07	2.31	0.83	2.22

TABLE S5: Trends of globally averaged precipitation in wet and dry seasons, and the annual precipitation range for the 18 CMIP5 climate model (Table S2) simulations in the RCP8.5 scenario, combined with the historical runs. One realization from each model is chosen. The unit is % per 1˚C. The period for calculating the trends is 1979-2010 for GPCP, GPCC and the model simulations, and 1979-2009 for CRU. Land precipitation shown here is averaged over those land areas with data, so land areas are slightly different among observations. The trends that passed the 95% statistical confidence level of a two-tailed t test are marked in bold font.

Model	**Wet**		**dry**		**annual range**	
coverage	global	Land	global	land	global	land
GPCP	**13.62**	4.66	**-38.95**	-3.83	**33.72**	7.26
CRU	——	**8.36**	——	**31.60**	——	6.46
GPCC	——	**8.83**	——	11.03	——	**10.34**
ensemble	**3.25**	**3.97**	-0.03	**1.75**	**3.92**	3.93
BBC-CSM1.1	**3.26**	0.53	0.81	3.75	**3.49**	-0.48
CanESM2	**3.10**	**2.80**	-2.40	-2.96	**4.38**	**3.43**
CCSM4	2.31	**2.96**	3.38	4.50	1.73	2.37
FGOALS-g2	**4.24**	**6.15**	-0.14	-2.02	**5.61**	**7.87**
FGOALS-s2	**2.84**	**5.92**	-0.80	1.39	**3.82**	**6.41**
GFDL-CM3	2.05	**3.43**	2.10	1.17	1.95	**3.64**
GFDL-ESM2G	**3.22**	1.21	-0.59	1.47	**3.89**	0.92
GFDL-ESM2M	3.32	5.18	-1.33	-1.85	4.19	**5.55**
GISS-E2-R	**2.54**	0.53	-0.04	3.75	3.80	-0.48
HadGEM2-CC	**4.83**	**9.31**	-1.20	2.57	5.57	**9.05**
INM-CM4	**5.54**	3.44	2.15	-1.40	4.40	3.27
IPSL-CM5A-LR	**2.82**	0.35	1.15	**3.57**	**3.08**	-0.34
MIROC5	**2.99**	**4.69**	0.42	**2.92**	**3.14**	**3.87**
MIROC5-ESM	**3.86**	**7.28**	-0.86	-0.87	**4.99**	**8.16**
MIROC5-ESM-CHEM	**2.65**	**9.64**	0.26	7.75	**3.54**	**10.47**
MPI-ESM-LR	**7.39**	**9.48**	-2.32	6.23	**8.64**	**8.09**
MRI-CGCM3	3.15	1.93	3.43	-1.87	2.23	2.19
NorESM1-M	3.21	1.40	-5.18	6.74	5.64	0.40

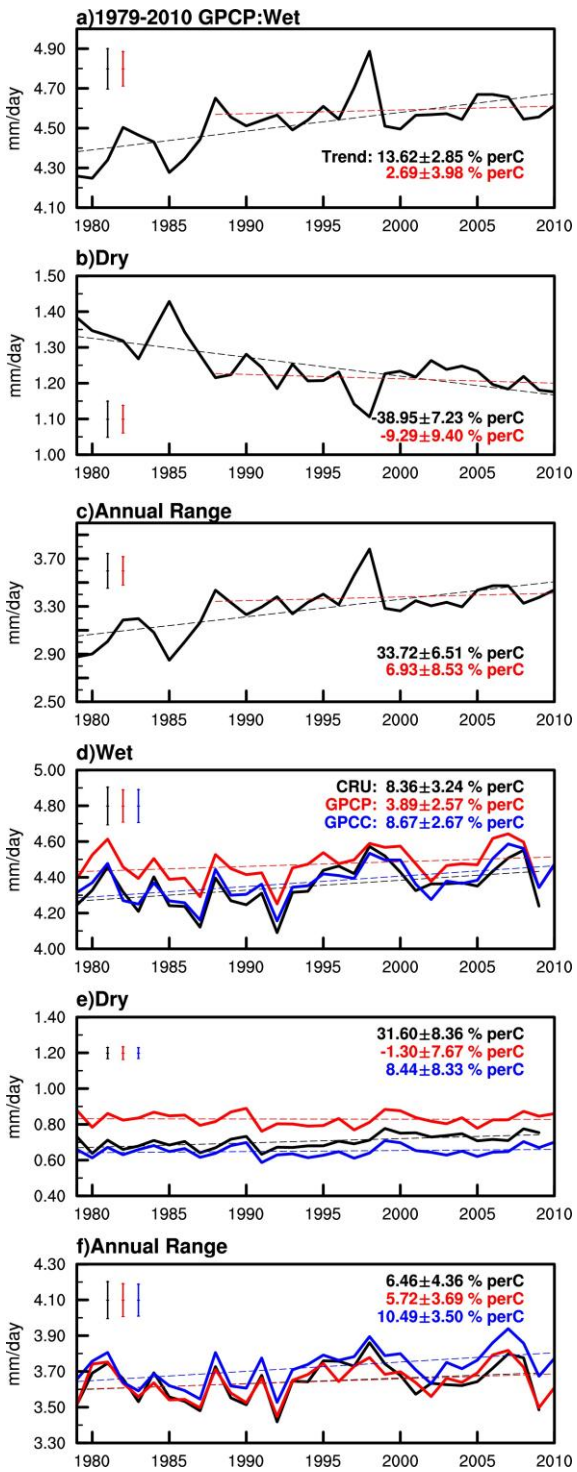

Figure S1 | Time series (1979-2010) of global averages of the GPCP precipitation (mm day^{-1}). **a**, Wet seasons, **b**, dry seasons, and **c**, the annual range. **d**, **e**, and **f**, As in **a**, **b**, and **c**, but for the CRU, GPCC and GPCP land precipitation. For consistency, CRU land is used in GPCC and GPCP. The dashed line is the linear least-square fit to the time series. The red (black) dashed line in **a**, **b** and **c** is for the period of 1979-2010 (1988-2010). The error bars at left are ±1 standard deviation for the corresponding detrended time series.

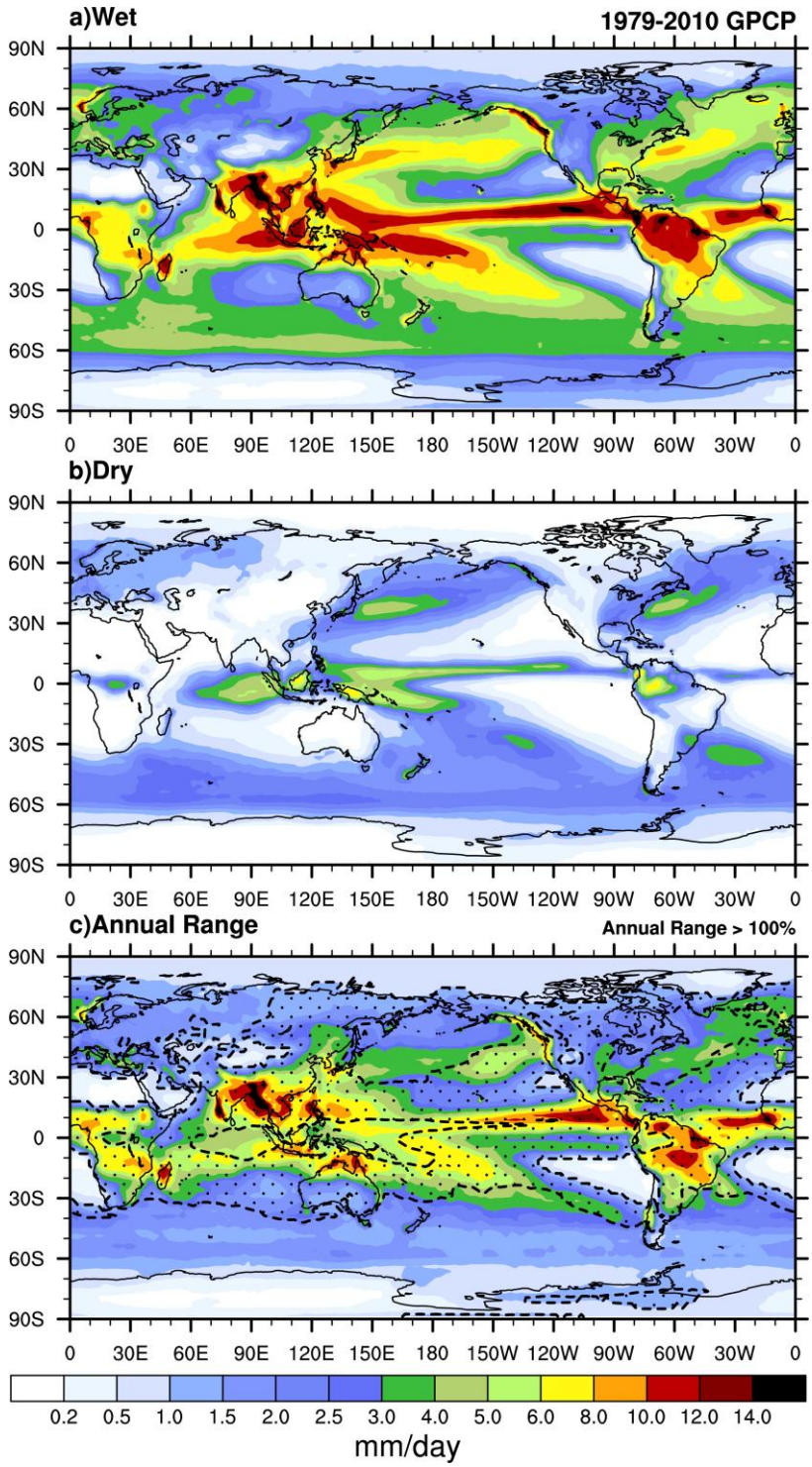

Figure S2 | Climatology (1979-2010) of the GPCP precipitation. a, Wet seasons, **b**, dry seasons, and **c**, the annual range of precipitation. Areas with a strong annual cycle (the annual range of precipitation is larger than 1 mm day^{-1} and 100% of annual mean precipitation) are stippled in **c**. The unit is mm day^{-1}.

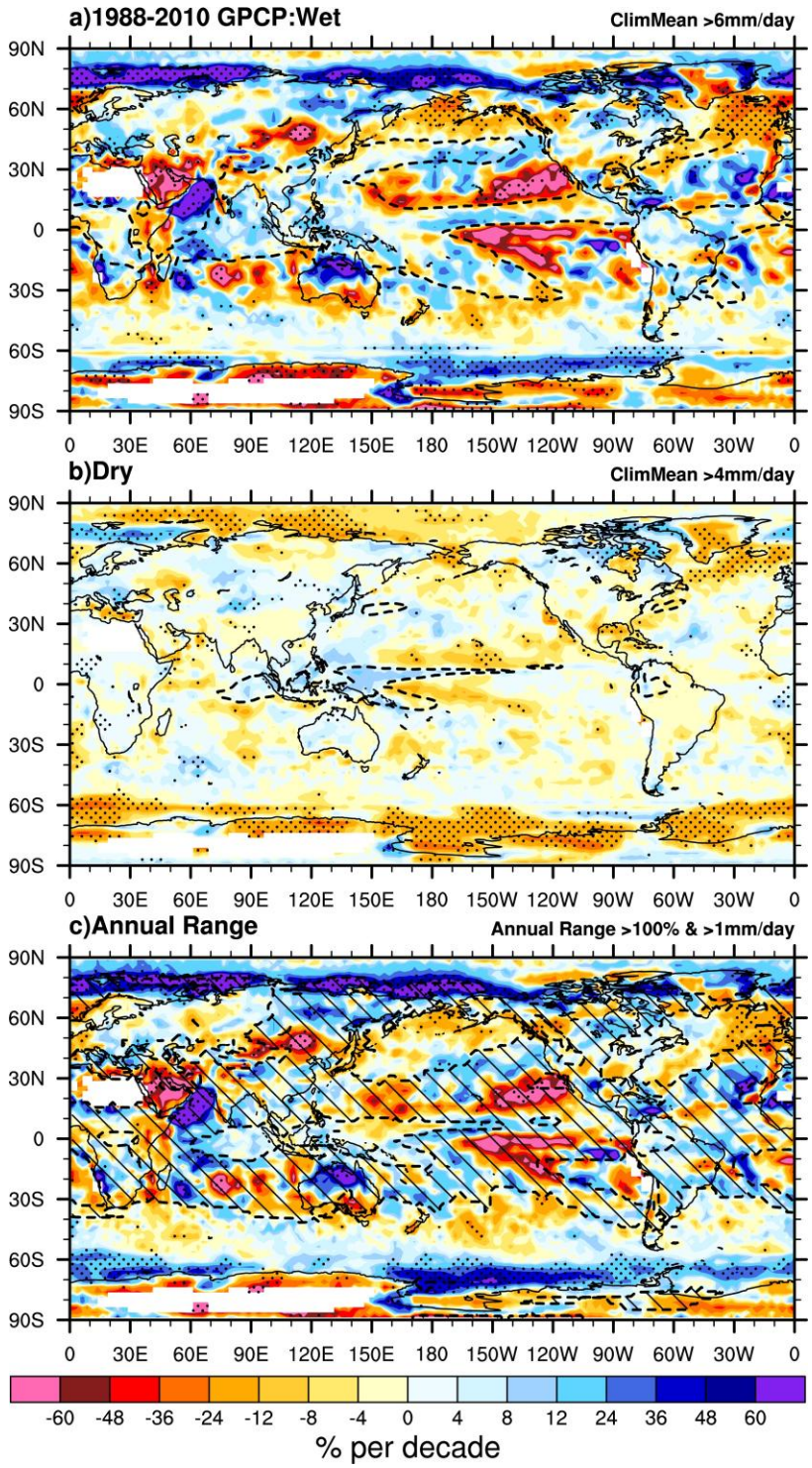

Figure S3 | Spatial distribution of linear trends in GPCP precipitation, 1988-2010. a, Wet seasons, **b**, dry seasons, and **c**, the annual range of precipitation. The unit is % decade^{-1}, which is the trend in mm day^{-1} decade^{-1} divided by annual climatology in each grid. Trends over areas with annual climatology less than 0.1 mm day^{-1} are not plotted, and those significant at the 95% statistical confidence level of a Students t test are stippled. The dashed curves indicate major convective zones, 6 mm day^{-1} for **a** and 4 mm day^{-1} for **b**. Regions with a strong annual cycle (the annual range of precipitation is larger than 1 mm day^{-1} and 100% of annual mean precipitation[7]) are hatched in **c**. The pattern correlations with the spatial distribution of trends in 1979-2010 (Fig. 2) are 0.70, 0.66 and 0.63 for wet seasons, dry seasons and the annual range, respectively.

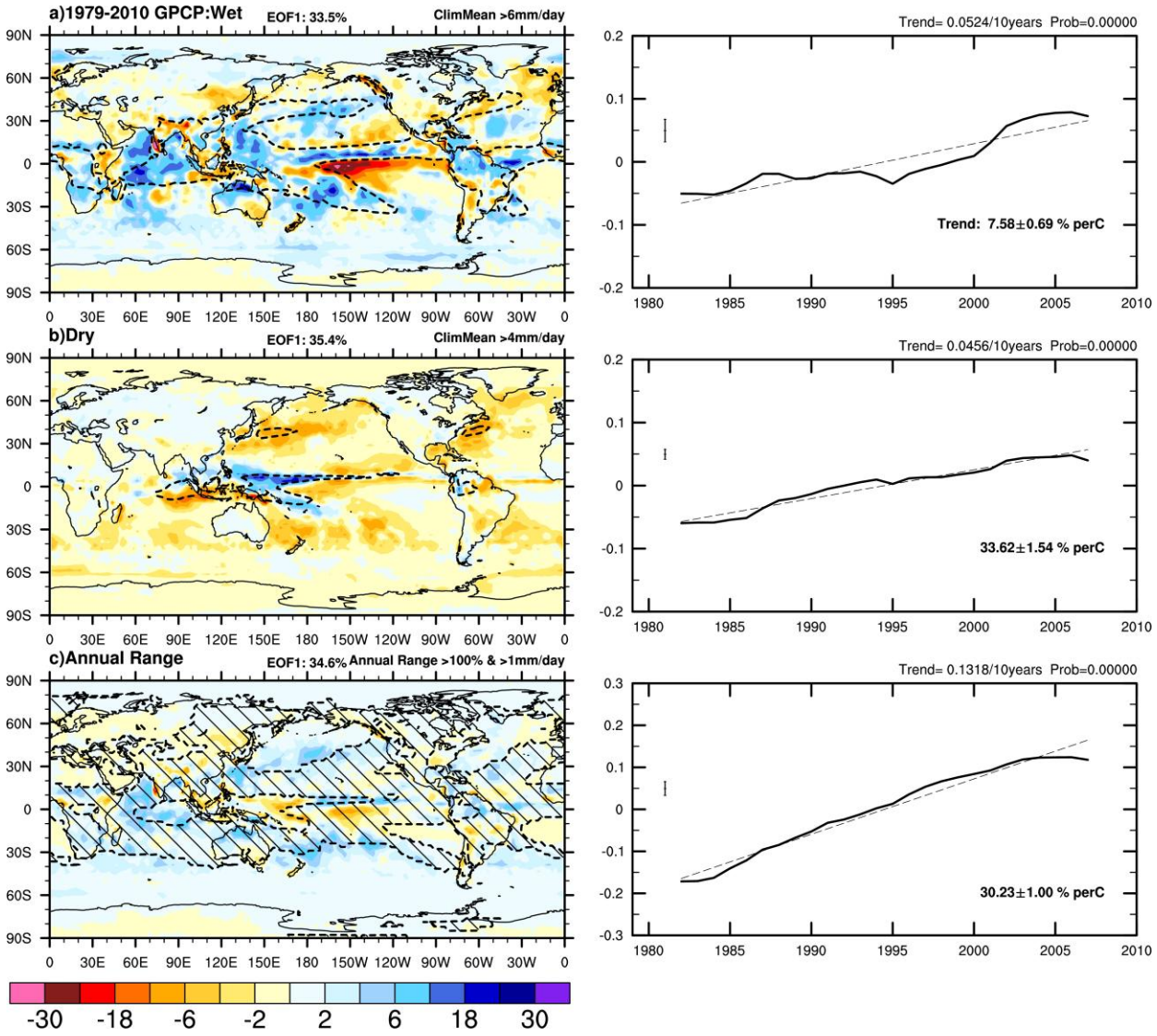

Figure S4 | The spatial distribution (left panels) and time series (right panels) of the first EOF of GPCP precipitation, 1979-2010. A seven-year running average is applied to the data prior to the EOF. **a**, Wet seasons, **b**, dry seasons, and **c**, the annual range of precipitation. 33.5%, 35.4% and 34.6% of variances are explained by the 1st EOF for wet seasons, dry seasons and the annual range, respectively. The unit in time series is mm day^{-1}.

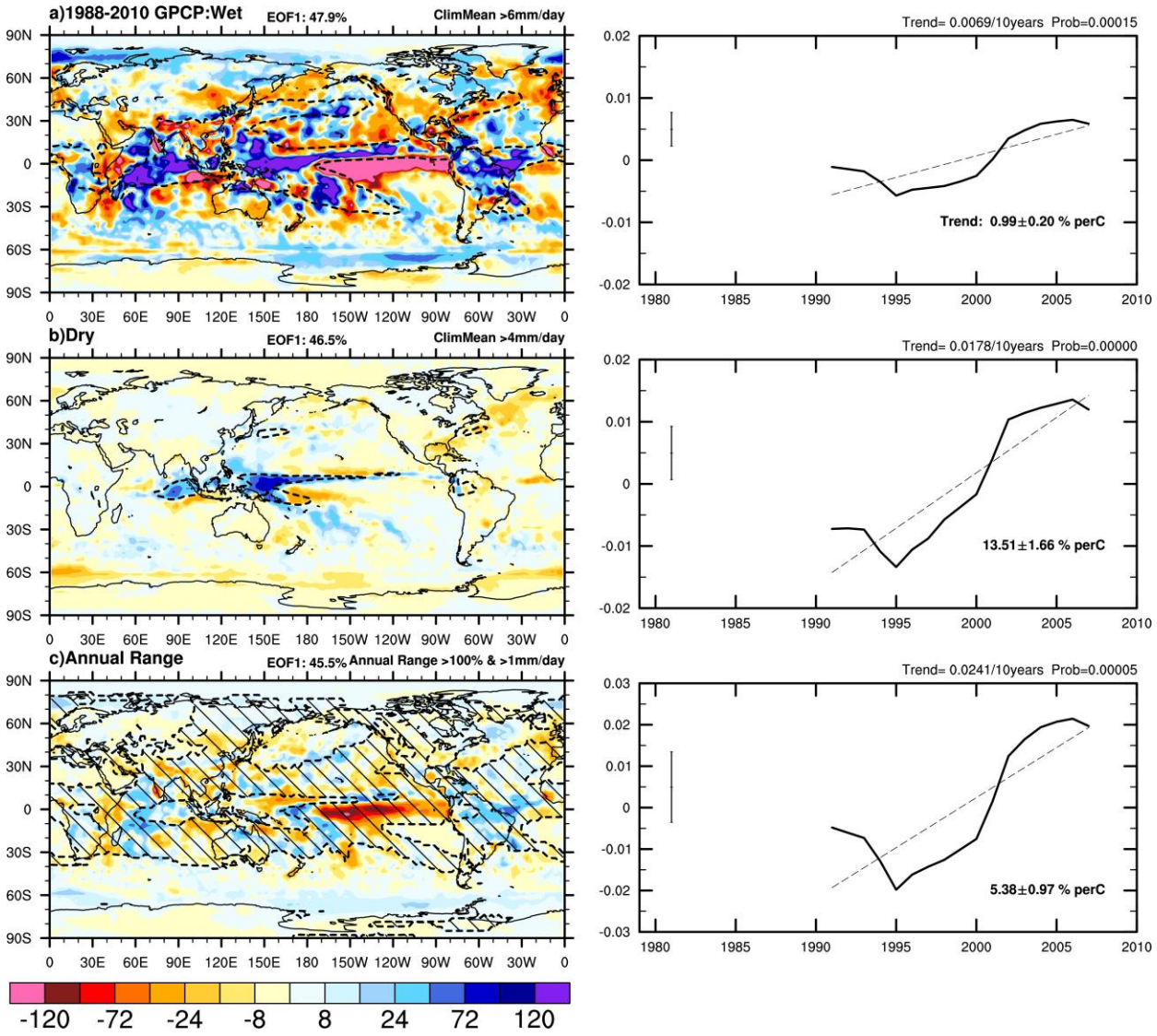

Figure S5 | The spatial distribution (left panels) and time series (right panels) of the first EOF of GPCP precipitation, 1988-2010. A seven-year running average is applied to the data prior to the EOF. **a**, Wet seasons, **b**, dry seasons, and **c**, the annual range of precipitation. 47.9%, 46.5% and 45.5% of variances are explained by the 1st EOF for wet seasons, dry seasons and the annual range, respectively. The unit in time series is mm day^{-1}.

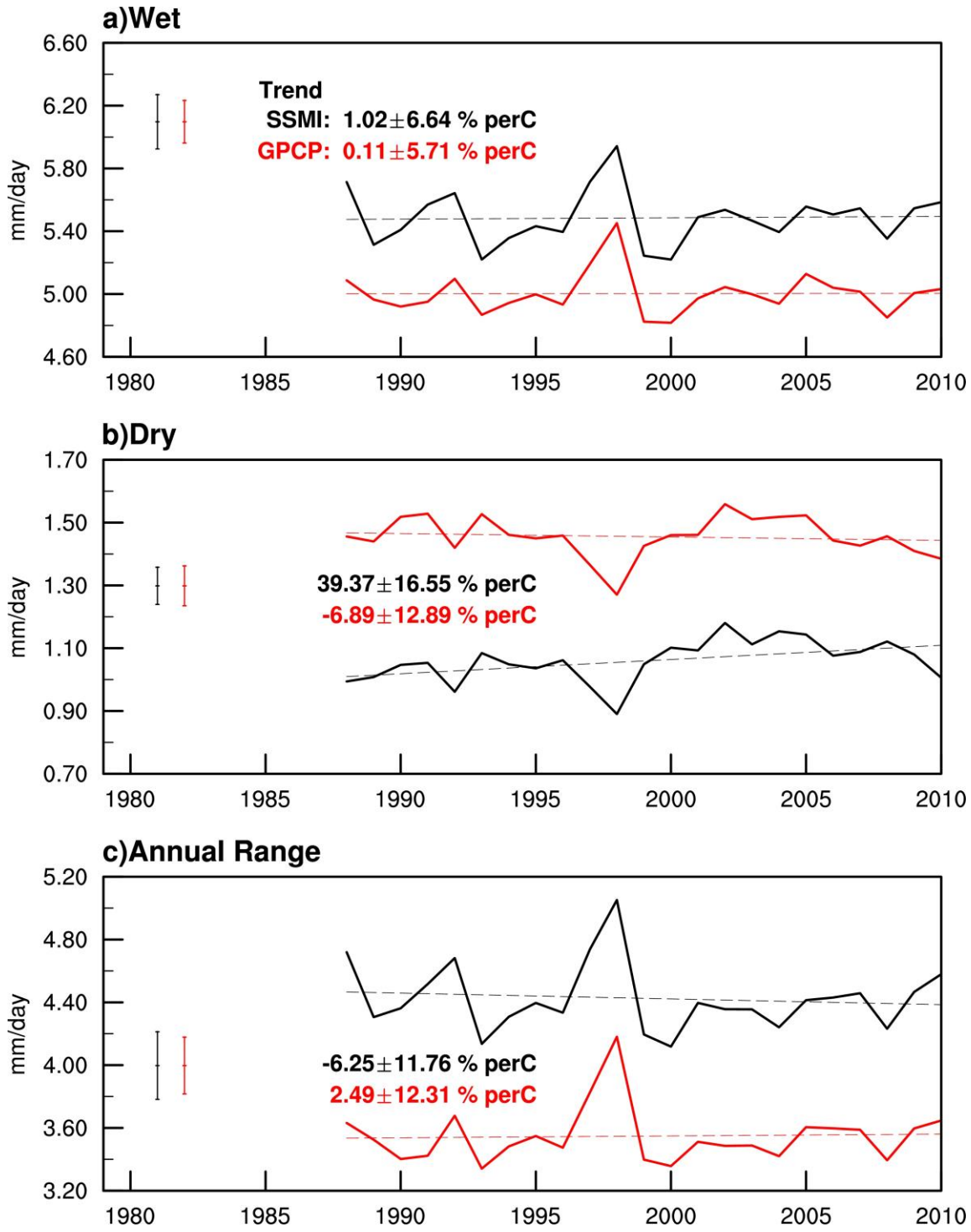

Figure S6 | Time series of global averages in SSM/I and GPCP ocean precipitation. a, Wet seasons, **b**, dry seasons, and **c**, the annual range of precipitation. For consistency, ocean areas used in GPCP are same as in SSM/I. The unit is mm day^{-1}. The error bars at top left are ±1 standard deviation with removing the linear trends. Top right is the trends for each data, with a unit of % per 1 ˚C.

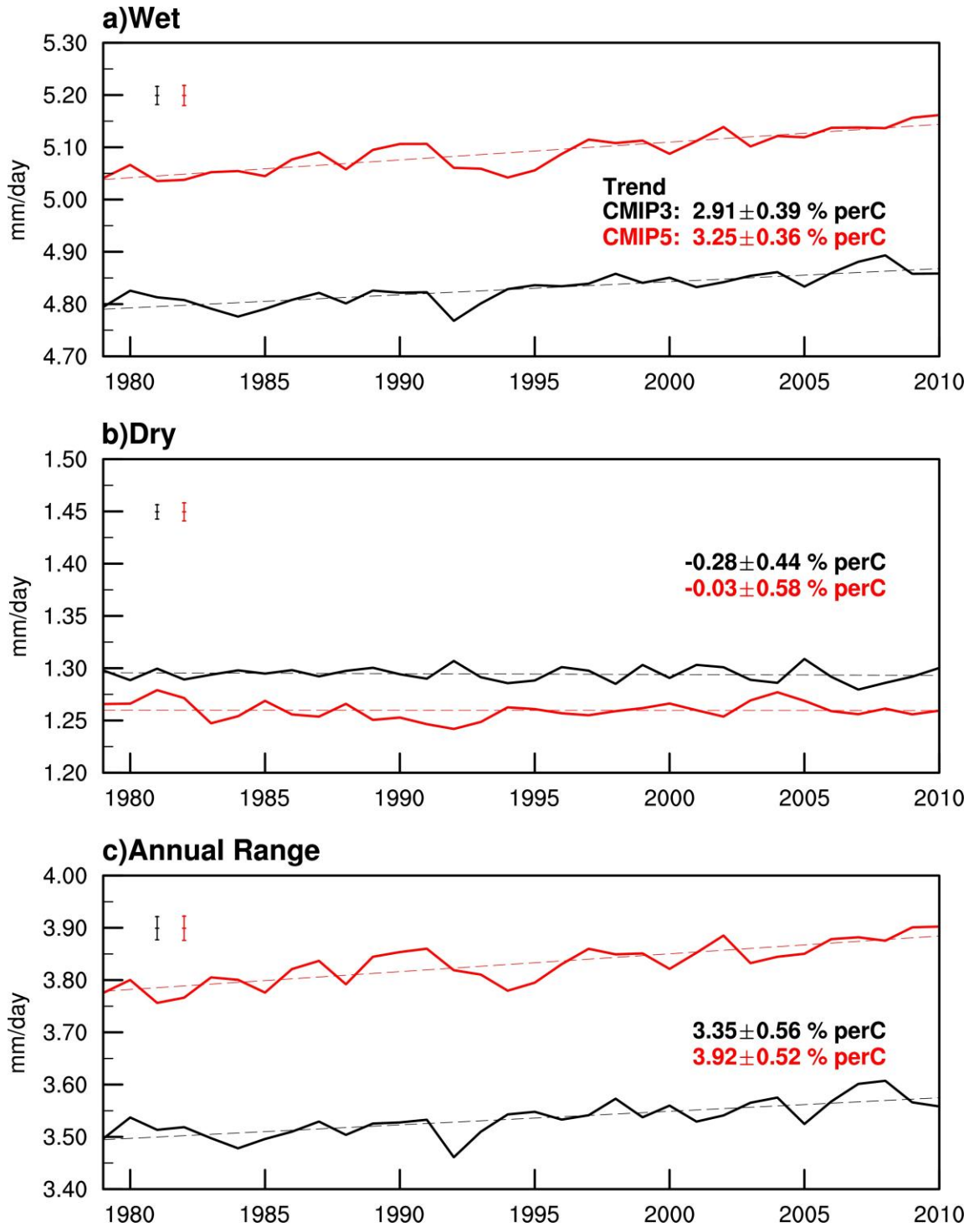

Figure S7 | Time series (1979-2010) for global averages of precipitation from the 23 CMIP3 (black) and 18 CMIP5 (red) multimodel ensembles. a, Wet seasons, **b**, dry seasons, and **c**, the annual range of precipitation. The unit is mm day^{-1}. The error bars at left are ±1 standard deviation for each multimodel ensemble.

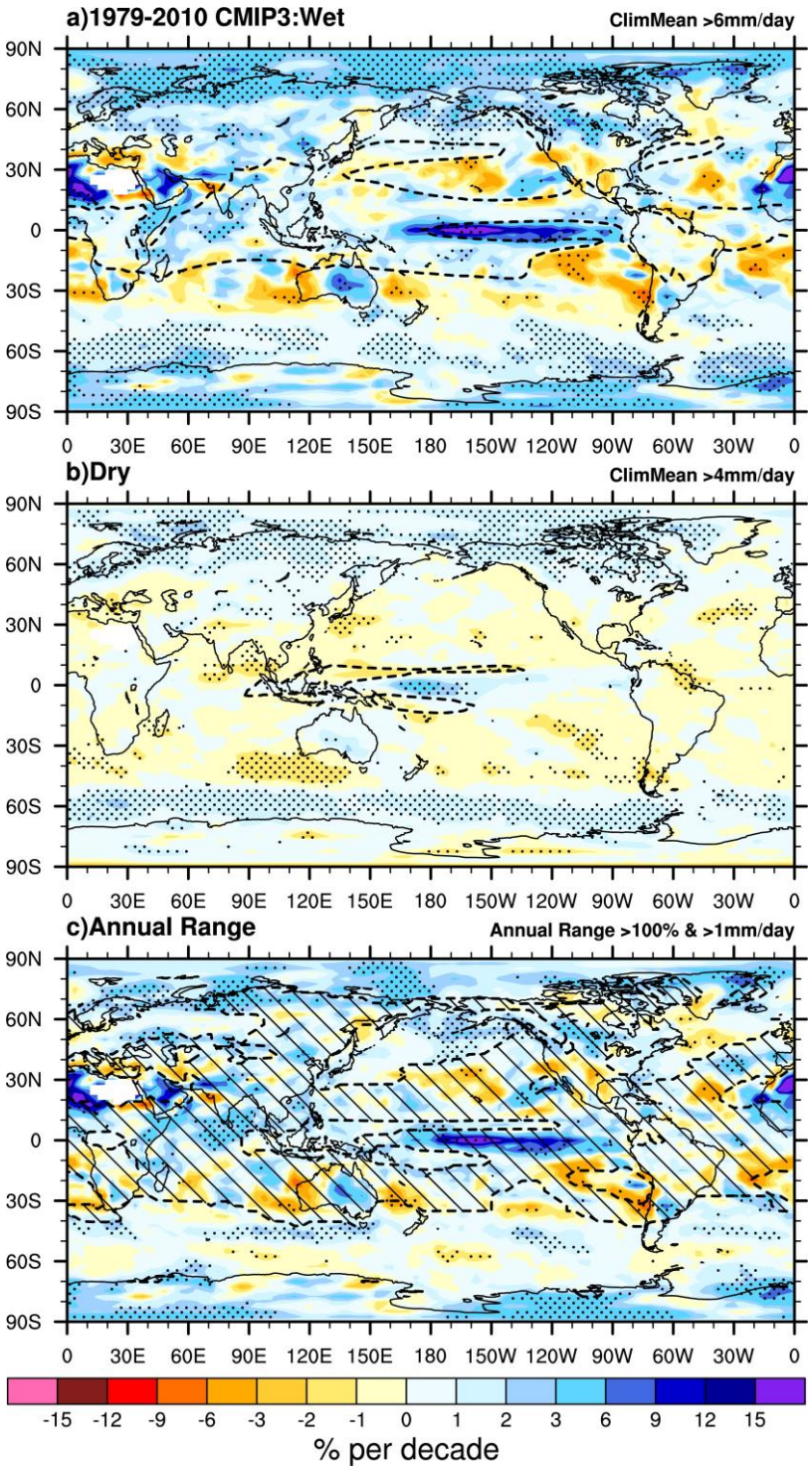

Figure S8 | Spatial distribution of linear trends in precipitation of the 23 CMIP3 multimodel (Table S1) ensemble mean, 1979-2010. a, Wet seasons, **b**, dry seasons, and **c**, the annual range of precipitation. The unit is % decade^{-1}. Trends that passed the 95% statistical confidence level of a Students t test are stippled. The dashed curves indicate major convective zones, 6 mm day^{-1} for **a** and 4 mm day^{-1} for **b**. Areas with a strong annual cycle are hatched.

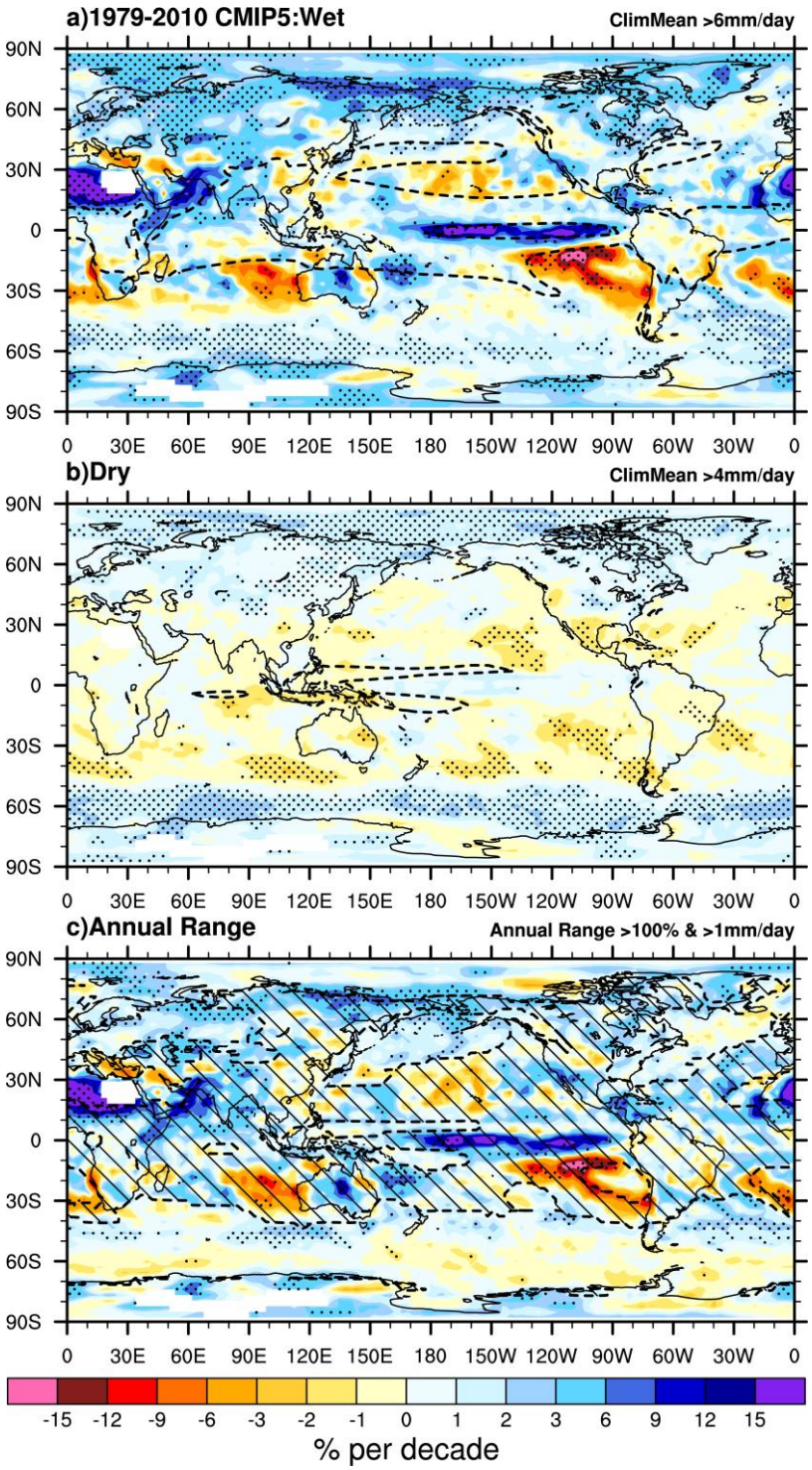

Figure S9 | Spatial distribution of linear trends in precipitation of the 18 CMIP5 multimodel (Table S2) ensemble mean, 1979-2010. a, Wet seasons, **b**, dry seasons, and **c**, the annual range of precipitation. The unit is % decade^{-1}. Trends that passed the 95% statistical confidence level of a Students t test are stippled. The dashed curves indicate major convective zones, 6 mm day^{-1} for **a** and 4 mm day^{-1} for **b**. Areas with a strong annual cycle are hatched.